Molecules **2004**, *9*, 1034-1052

molecules

ISSN 1420-3049
http://www.mdpi.org

Application of 'Inductive' QSAR Descriptors for Quantification of Antibacterial Activity of Cationic Polypeptides

Artem Cherkasov [1,*] and Bojana Jankovic [2]

[1] Division of Infectious Diseases, Faculty of Medicine, University of British Columbia, 2733 Heather Street, Vancouver, BC, V5Z 3J5, Canada, Tel.: (+1) 604-875-4111 x 68541; Fax: (+1) 604-875-4013
[2] BC Cancer Research Centre, 601 West 10th Avenue, Vancouver, BC, V5Z 4E6, Canada. Tel.: (+1) 604-877-6010 x 3189; Email: bojana_jankovic@shaw.ca

* Author to whom correspondence should be addressed: e-mail: artc@interchange.ubc.ca

Received: 25 May 2004 / Accepted: 14 June 2004 / Published: 31 December 2004

Abstract: On the basis of the inductive QSAR descriptors we have created a neural network-based solution enabling quantification of antibacterial activity in the series of 101 synthetic cationic polypeptides (CAMEL-s). The developed QSAR model allowed 80% correct categorical classification of antibacterial potencies of the CAMEL-s both in the training and the validation sets. The accuracy of the activity predictions demonstrates that a narrow set of 3D sensitive 'inductive' descriptors can adequately describe the aspects of intra- and intermolecular interactions that are relevant for antibacterial activity of the cationic polypeptides. The developed approach can be further expanded for the larger sets of biologically active peptides and can serve as a useful quantitative tool for rational antibiotic design and discovery.

Keywords: QSAR, inductive descriptors, antibacterial peptides, antibiotics.

Introduction

QSAR models for antibiotic activity

QSAR studies of antibiotic activity represent an emerging and exceptionally important topic in the area of computed-aided drug design. Although the demand for '*in silico*' discovery is clear in all areas of human therapeutics, the field of anti-infective drugs has a particular need for computational

solutions enabling rapid identification of novel therapeutic leads. As a result, there is an urge for new antibiotics and antivirals driven by critical situations, such as the increased prevalence of multi-drug resistant bacteria and HIV/AIDS, and the emergence or re-emergence of deadly infectious diseases such as Lyme disease, West Nile virus, Hantavirus pulmonary syndrome, Norwalk-like virus, Avian influenza virus, SARS, and novel forms of Cryptococcal infection. On another hand, historically, 'Big Pharma' have withdrawn from the field of antimicrobial drug development in favour of more profitable areas. Consequently, very few novel antibacterial therapeutics have emerged over the last decade. At this moment, QSAR studies can help solving this problem by providing the means of rapid design and virtual screening of combinatorial anti-infective libraries, as well as for rational data mining for novel antibiotic candidates.

Few antibacterial QSAR studies have been reported up to date, which could either distinguish compounds possessing antibacterial activity from all other chemicals, or numerically reproduce antibacterial potencies in the series of closely related chemical analogues. These QSAR approaches process a variety of structure-dependent descriptors with machine learning and statistical techniques such as Artificial Neural Networks [1-3], Linear Discriminant Analysis, [4-6] Binary Logistic Regression [5], Principal Component Analysis and *k*-means Cluster method [7]. In some cases the results allowed the authors to introduce novel anti-infective leads, however, all of the reported QSAR solutions have been built upon already well - studied classes of traditional antibiotics. In the current work, we apply the QSAR methodology to the newest class of antibacterial therapeutics – the cationic polypeptides, which represent the latest hope in the combat against multi-drug resistant pathogens.

Cationic polypeptides as a novel class of antibacterial therapeutics

A diverse population of antimicrobial peptides (AMP-s) can be found in nature, as they are an essential component of anti-infective defence mechanisms in mammals, amphibians, insects and plants [8-11]. The majority of AMP-s share several key structural features such as short length (typically 10 to 40 amino acids), amphipathicity (*i.e.,* a molecule has distinct cationic and hydrophobic faces), and helical or cyclic structure. In the recent years, AMP-s have drawn much attention as a potentially effective class of anti-infectious therapeutics. Considering the facts that bacterial resistance to antimicrobial peptides is infrequent [12, 13, 8], they are non-toxic and non-immunogenic (according to numerous reports, such as [14]), extensive research programs have been established with the aim to exploit the AMP-s as a novel stand-alone class of antibiotics.

Substantial experimental efforts have been invested into discovery and investigation of natural and synthetic cationic polypeptides possessing antibacterial, antiviral, antifungal and/or anti-tumour activities. Nevertheless, only a few very simple structure-activity studies have been reported in the literature, with the results not leading to validated QSAR models. In the current work, we have attempted to fill this gap by creating a QSAR model quantifying antibacterial activity of a broad range of rigorously investigated cationic peptides through the recently developed 'inductive' QSAR descriptors.

'Inductive' descriptors overview

The 'inductive' descriptors have been previously introduced, and are based on the models of inductive and steric effects, inductive electronegativity and molecular capacitance, developed in a series of papers by Cherkasov and co-authors [15-19]. These molecular parameters can be easily accessed from fundamental parameters of bound atoms, such as absolute electronegativities (χ), covalent radii (R) and intramolecular distances (r). The steric *Rs* and inductive *σ** influence of *n* - atomic group *G* on a single atom *j* is:

$$Rs_{G\to j} = \alpha \sum_{i\subset G, i\neq j}^{n} \frac{R_i^2}{r_{i-j}^2} \tag{1}$$

$$\sigma^*_{G\to j} = \beta \sum_{i\subset G, i\neq j}^{n} \frac{(\chi_i^0 - \chi_j^0)R_i^2}{r_{i-j}^2} \tag{2}$$

In those cases when the inductive and steric interactions occur between a given atom *j* and the rest of *N*-atomic molecule (as sub-substituent), the summation in (1) and (2) is taken over N-1 terms. Thus, the group electronegativity of *(N-1)*-atomic substituent around atom *j* is expressed as the following:

$$\chi^0_{N-1\to j} = \frac{\sum_{i\neq j}^{N-1} \frac{\chi_i^0 (R_i^2 + R_j^2)}{r_{i-j}^2}}{\sum_{i\neq j}^{N-1} \frac{R_i^2 + R_j^2}{r_{i-j}^2}} \tag{3}$$

Similarly, steric and inductive effects of a singe atom onto a group of atoms (the rest of the molecule) are defined as:

$$Rs_{j\to N-1} = \alpha \sum_{i\neq j}^{N-1} \frac{R_j^2}{r_{j-i}^2} = \alpha R_j^2 \sum_{i\neq j}^{N-1} \frac{1}{r_{j-i}^2} \tag{4}$$

$$\sigma^*_{j\to N-1} = \beta \sum_{i\neq j}^{N-1} \frac{(\chi_j^0 - \chi_i^0)R_j^2}{r_{j-i}^2} = \beta R_j^2 \sum_{i\neq j}^{N-1} \frac{(\chi_j^0 - \chi_i^0)}{r_{j-i}^2} \tag{5}$$

In the work [18] an iterative procedure for calculating a partial charge on *j-th* atom in a molecule was developed, and it is:

$$\Delta N_j = Q_j + \gamma \sum_{i\neq j}^{N-1} \frac{(\chi_j - \chi_i)(R_j^2 + R_i^2)}{r_{j-i}^2} \tag{6}$$

(where Q_j reflects the formal charge of an toms *j*).

Initially, the parameter χ in (6) corresponds to χ^0 - an absolute, unchanged electronegativity of an atom As the iterative calculation progresses, the equalized electronegativity χ' gets updated according to (7):

$$\chi' \approx \chi^0 + \eta^0 \Delta N \tag{7}$$

where the local chemical hardness η^0 reflects the "resistance" of electronegativity to a change of the atomic charge. The 'inductive' hardness η_i and softness s_i of a bound atom *i* are represented in the following manner:

$$\eta_i = \frac{1}{2\sum_{j\neq i}^{N-1} \frac{R_j^2 + R_i^2}{r_{j-i}^2}} \tag{8}$$

$$s_i = 2\sum_{j\neq i}^{N-1} \frac{R_j^2 + R_i^2}{r_{j-i}^2} \quad (9)$$

The corresponding group parameters are therefore expressed as:

$$\eta_{MOL} = \frac{1}{s_{MOL}} = \frac{1}{2\sum_{j\neq i}^{N-1} \frac{R_j^2 + R_i^2}{r_{j-i}^2}} \quad (10)$$

$$s_{MOL} = \sum_{j\neq i}^{N}\sum_{j\neq i}^{N} \frac{R_j^2 + R_i^2}{r_{j-i}^2} = \sum_{j\neq i}^{N} 2\frac{R_j^2 + R_i^2}{r_{j-i}^2} = \sum_{i}^{N} s_i \quad (11)$$

The interpretation of the physical meaning of the 'inductive' descriptors was developed by considering a neutral molecule as an electrical capacitor formed by charged atomic spheres [18]. This approximation relates chemical softness-hardness of bound atom(s) with the areas of the facings of an electrical capacitor radically formed by the atom(s) in a molecule (Figure 1), and correlates electronic density with capacitor-accumulated electricity.

Figure 1. Radial shielding on spherical surface of atom A by the neighbouring atom B

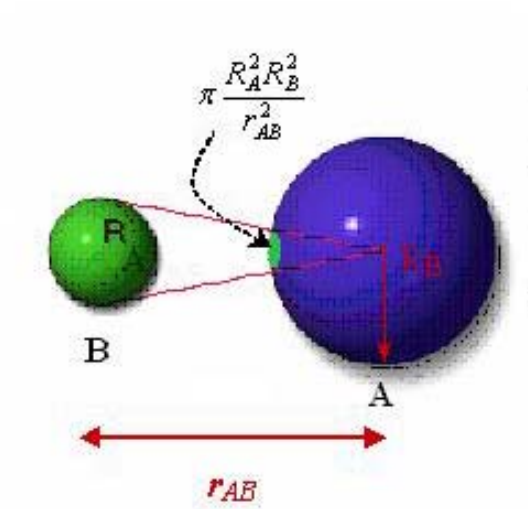

The area of a frontal of a surface of atom A by atom B (shown as a green shadow) is $\pi \frac{R_1^2 R_B^2}{r_{AB}^2}$.

The entire area A is πR_A^2, thus the relative screened surface of A can be determined as $\frac{S_{shadow}}{S_{atom}} = \frac{\pi R_1^2 R_B^2}{\pi R_1^2 r_{AB}^2} = \frac{R_B^2}{r_{AB}^2}$.

The validation of Cherkasov's 'inductive' parameters, developed to date, has been rigorously conducted on extensive experimental datasets [15-24]. Table 1 features 50 'inductive' QSAR descriptors that can be calculated in the framework of equations (1)-(11). It should be noted that in a previous study [25], these molecular parameters allowed creation of the QSAR model enabling 93% correct recognition of low-molecular weight antibacterial compounds.

Table 1. Inductive QSAR descriptors introduced on the basis of equations (1)-(11).

Descriptor	Characterization	Parental formula(s)
χ (electronegativity) – based		
EO_Equalized*	Iteratively equalized electronegativity of a molecule	Calculated iteratively by (7) where charges get updated according to (6); an atomic hardness in (7) is expressed through (8)
Average_EO_Pos*	Arithmetic mean of electronegativities of atoms with positive partial charge	$\frac{\sum_i^{n^+} \chi_i^0}{n^+}$ where n^+ is the number of atoms *i* in a molecule with positive partial charge
Average_EO_Neg*	Arithmetic mean of electronegativities of atoms with negative partial charge	$\frac{\sum_i^{n^-} \chi_i^0}{n^-}$ where n^- is the number of atoms *i* in a molecule with negative partial charge
η (hardness) – based		
Global_Hardness	Molecular hardness - reversed softness of a molecule	(10)
Sum_Hardness*	Sum of hardnesses of atoms of a molecule	Calculated as a sum of inversed atomic softnesses in turn computed within (9)
Sum_Pos_Hardness	Sum of hardnesses of atoms with positive partial charge	Obtained by summing up the contributions from atoms with positive charge computed by (8)
Sum_Neg_Hardness	Sum of hardnesses of atoms with negative partial charge	Obtained by summing up the contributions from atoms with negative charge computed by (8)
Average_Hardness*	Arithmetic mean of hardnesses of all atoms of a molecule	Estimated by dividing quantity (10) by the number of atoms in a molecule
Average_Pos_Hardness*	Arithmetic mean of hardnesses of atoms with positive partial charge	$\frac{\sum_i^{n^+} \eta_i}{n^+}$ where n^+ is the number of atoms *i* with positive partial charge.
Average_Neg_Hardness*	Arithmetic mean of hardnesses of atoms with negative partial charge	$\frac{\sum_i^{n^-} \eta_i}{n^-}$ where n^- is the number of atoms *i* with negative partial charge.
Smallest_Pos_Hardness	Smallest atomic hardness among values for positively charged atoms	(8)
Smallest_Neg_Hardness	Smallest atomic hardness among values for negatively charged atoms.	(8)
Largest_Pos_Hardness*	Largest atomic hardness among values for positively charged atoms	(8)

Table 1. Cont.

Descriptor	Characterization	Parental formula(s)
Largest_Neg_Hardness*	Largest atomic hardness among values for negatively charged atoms	(8)
Hardness_of_Most_Pos*	Atomic hardness of an atom with the most positive charge	(8)
Hardness_of_Most_Neg	Atomic hardness of an atom with the most negative charge	(8)
s (softness) – based		
Global_Softness	Molecular softness – sum of constituent atomic softnesses	(11)
Total_Pos_Softness	Sum of softnesses of atoms with positive partial charge	Obtained by summing up the contributions from atoms with positive charge computed by (9)
Total_Neg_Softness*	Sum of softnesses of atoms with negative partial charge	Obtained by summing up the contributions from atoms with negative charge computed by (9)
Average_Softness	Arithmetic mean of softnesses of all atoms of a molecule	(11) divided by the number of atoms in molecule
Average_Pos_Softness	Arithmetic mean of softnesses of atoms with positive partial charge	$\frac{\sum_i^{n^+} s_i}{n^+}$ where n^+ is the number of atoms i with positive partial charge.
Average_Neg_Softness	Arithmetic mean of softnesses of atoms with negative partial charge	$\frac{\sum_i^{n^-} s_i}{n^-}$ where n^- is the number of atoms i with negative partial charge.
Smallest_Pos_Softness	Smallest atomic softness among values for positively charged atoms	(9)
Smallest_Neg_Softness	Smallest atomic softness among values for negatively charged atoms	(9)
Largest_Pos_Softness	Largest atomic softness among values for positively charged atoms	(9)
Largest_Neg_Softness	Largest atomic softness among values for positively charged atoms	(9)
Softness_of_Most_Pos	Atomic softness of an atom with the most positive charge	(9)
Softness_of_Most_Neg	Atomic softness of an atom with the most negative charge	(9)
q (charge)- based		
Total_Charge	Sum of absolute values of partial charges on all atoms of a molecule	$\sum_i^N \lvert\Delta N_i\rvert$ where all the contributions ΔN_i derived within (6)
Total_Charge_Formal*	Sum of charges on all atoms of a molecule (formal charge of a molecule)	Sum of all contributions (6)

Table 1. Cont.

Descriptor	Characterization	Parental formula(s)
Average_Pos_Charge*	Arithmetic mean of positive partial charges on atoms of a molecule	$\frac{\sum_{i}^{n^+}\Delta N_i}{n^+}$ where n^+ is the number of atoms *i* with positive partial charge
Average_Neg_Charge*	Arithmetic mean of negative partial charges on atoms of a molecule	$\frac{\sum_{i}^{n^-}\Delta N_i}{n^-}$ where n^- is the number of atoms *i* with negative partial charge
Most_Pos_Charge*	Largest partial charge among values for positively charged atoms	(6)
Most_Neg_Charge	Largest partial charge among values for negatively charged atoms	(6)
σ (inductive parameter) – based*		
Total_Sigma_mol_i	Sum of inductive parameters *σ*(molecule→atom)* for all atoms within a molecule	$\sum_{i}^{N}\sigma^*_{G\to i}$ where contributions $\sigma^*_{G\to i}$ are computed by equation (2) with *n=N-1* – i.e. each atom *j* is considered against the rest of the molecule *G*
Total_Abs_Sigma_mol_i	Sum of absolute values of group inductive parameters *σ*(molecule→atom)* for all atoms within a molecule	$\sum_{i}^{N}\left\|\sigma^*_{G\to i}\right\|$
Most_Pos_Sigma_mol_i*	Largest positive group inductive parameter *σ*(molecule→atom)* for atoms in a molecule	(2)
Most_Neg_Sigma_mol_i	Largest (by absolute value) negative group inductive parameter *σ*(molecule→atom)* for atoms in a molecule	(2)
Most_Pos_Sigma_i_mol	Largest positive atomic inductive parameter *σ*(atom→molecule)* for atoms in a molecule	(5)
Most_Neg_Sigma_i_mol*	Largest negative atomic inductive parameter *σ*(atom→molecule)* for atoms in a molecule	(5)
Sum_Pos_Sigma_mol_i	Sum of all positive group inductive parameters *σ*(molecule →atom)* within a molecule	$\sum_{i}^{n^+}\left\|\sigma^*_{G\to i}\right\|$ where $\sigma^*_{G\to i}>0$ and n^+ is the number of *N-1* atomic substituents in a molecule with positive inductive effect (electron acceptors)
Sum_Neg_Sigma_mol_i*	Sum of all negative group inductive parameters *σ*(molecule →atom)* within a molecule	$\sum_{i}^{n^-}\left\|\sigma^*_{G\to i}\right\|$ where $\sigma^*_{G\to i}<0$ and n^- is the number of *N-1* atomic substituents in a molecule with negative inductive effect (electron donors)

Table 1. Cont.

Descriptor	Characterization	Parental formula(s)
Rs (steric parameter) – based		
Largest_Rs_mol_i	Largest value of steric influence *Rs(molecule→atom)* in a molecule	(1) where *n=N-1* - each atom *j* is considered against the rest of the molecule *G*
Smallest_Rs_mol_i*	Smallest value of group steric influence *Rs(molecule→atom)* in a molecule	(1) where *n=N-1* - each atom *j* is considered against the rest of the molecule *G*
Largest_Rs_i_mol	Largest value of atomic steric influence *Rs(atom→molecule)* in a molecule	(4)
Smallest_Rs_i_mol	Smallest value of atomic steric influence *Rs(atom→molecule)* in a molecule	(4)
Most_Pos_Rs_mol_i	Steric influence *Rs(molecule→atom)* ON the most positively charged atom in a molecule	(1)
Most_Neg_Rs_mol_i*	Steric influence *Rs(molecule→atom)* ON the most negatively charged atom in a molecule	(1)
Most_Pos_Rs_i_mol	Steric influence *Rs(atom→molecule)* OF the most positively charged atom to the rest of a molecule	(4)
Most_Neg_Rs_i_mol	Steric influence *Rs(atom→molecule)* OF the most negatively charged atom to the rest of a molecule	(4)

* *– descriptors selected for building the antibiotic peptide QSAR model.*

Results and Discussion

Experimental data

In the current work, we have used the 'inductive' descriptors to investigate structure-activity relationships in a series of antibiotic peptides called CAMEL-s. These compounds represent derivatives from the hybrid polypeptide CAMEL0 previously created by the respective fusion of the C- and N-terminus sequences of natural peptides Cecropin and Melittin. Despite the rather limited variability in amino acid sequences among these leucine-rich peptides, their antibacterial activity ranges over several orders of magnitude. It has been experimentally demonstrated that the CAMEL-s exhibit high activity against various strains (including the drug-resistant ones) of Gram-positive and Gram-negative bacteria, including *Bacteroides, Bordetella, Campylobacter, Corynebacterium, Klebsiella, Listeria, Moraxella, Pastuerella, Taylorella, Yersinia, Rhodococcus, Staphylococcus* and *Streptococcus* [26-28]. The minimal inhibitory concentrations for the series of 101 CAMEL-s against the listed microorganisms have been previously averaged to produce the mean antibiotic potency

parameters [26-28]. These values extracted from the SAPD database [29] have been collected into Table 2 and subjected to QSAR analysis with the 'inductive' descriptors.

Factors governing bioactivity of CAMEL-s

The common mode of action of antimicrobial peptides is disruption of bacterial cell membranes via electrostatic and hydrophobic interactions [1,3,4,12,14,29-36]. It is believed that amphipatic peptides can penetrate or form pores in the cell membranes through the insertion into the lipid bilayer mediated by hydrophobic forces, while their electrostatic interaction with phospholipid headgroups leads to membrane disruption. Cationic peptides exhibit high affinity only toward negatively charged surfaces of bacterial cells while they do not tend to interact with eukaryotic cells surfaces composed mostly of zwitterionic phospholipids. It has been demonstrated that antimicrobial activity of polypeptides can be influenced by their helicity, hydrophobicity and amphipathicity [5, 37-44]. Nonetheless, the exact nature of this correlation is still unclear and the understanding of the factors influencing the AMP activity is incomplete. We postulate that a set of the developed 'inductive' descriptors can adequately reflect those structure-dependent properties of CAMEL-s pertaining to their antibacterial activity. The reasoning for this stems from the fact that the parameters calculated within (1)–(11) cover a very broad range of proprieties of bound atoms and molecules related to their size, polarizability, electronegativity, compactness, mutual inductive and steric influence and distribution of electronic density, *etc*.

Descriptors calculation and selection

All 50 inductive QSAR descriptors (presented in detail in Table 1) have been calculated for all 101 CAMEL molecules under study. To compute the 'inductive' descriptors we have used the custom SVL-scripts implemented in the MOE package [45]. It should be noted that all of the produced parameters are 3D-sensitive and depend on the structure of polypeptides. The CAMEL-s were initially built in the alpha-helical conformations (the helicity was confirmed by a number of secondary structure predictors) which were further optimized by the MMFF9f molecular mechanic simulations.

It should be mentioned here, that some inductive descriptors may reflect related or similar molecular/atomic properties and can be correlated in certain cases (even though the analytical representation of those descriptors does not directly imply their co-linearity). Moreover, most of the CAMEL-s have very similar three-dimensional structures and, therefore, special precautions were taken in selecting the appropriate 'inductive' descriptors for the QSAR model. Hence, to eliminate the cross-correlation among the independent variables, we pre-computed pairwise regressions between all pairs of the 50 QSAR parameters for CAMEL-s. We subsequently removed those descriptors that linearly correlated with $R \geq 0.9$. As a result of this procedure, only 20 parameters were selected for further simulation (for more information refer to the Legend of Table 1). The descriptors are: Average Electronegativities of the Negatively/Positively Charged Atoms, Molecular (equalized) Electronegativity, Total Formal Charge, Average Atomic Hardness, Sum of Atomic Hardnesses, Average Negative/Positive Charges, Largest Positive Charge, Average Atomic Hardnesses of Negatively/Positively Charged Atoms, Hardness of the Most Positively Charged Atom, Largest Hardness among the Negatively/Positively Charged Atoms, Sum of Softnesses of Negatively Charged

Atoms, Steric Effect on the Most Negatively Charged Atom, Most Negative Inductive Constant of an Atom in Molecule, Largest Positive Inductive Effect on an Atom in Molecule, The Smallest Steric Effect on a Atom in Molecule, Sum of all Negative Inductive Effects on Atoms in Molecule.

The averaged values of these 20 indices were also separately calculated for antibacterial CAMEL-s conventionally sub-divided into three activity groups: very active (with the mean potency above 4), mild (potency between 2 and 4) and moderate antibacterials (potency < 2). The 'inductive' descriptors averaged within these three groups are plotted in Figure 2. Although the curves for moderate and very active peptides are very close for the most part, all three categories of CAMEL-s can be clearly distinguished by the selected QSAR parameters.

Figure 2. Distribution of the averaged values of the 'inductive' indices among 'Very active', 'Moderately active' and 'Mild' CAMEL polypeptides under investigation.

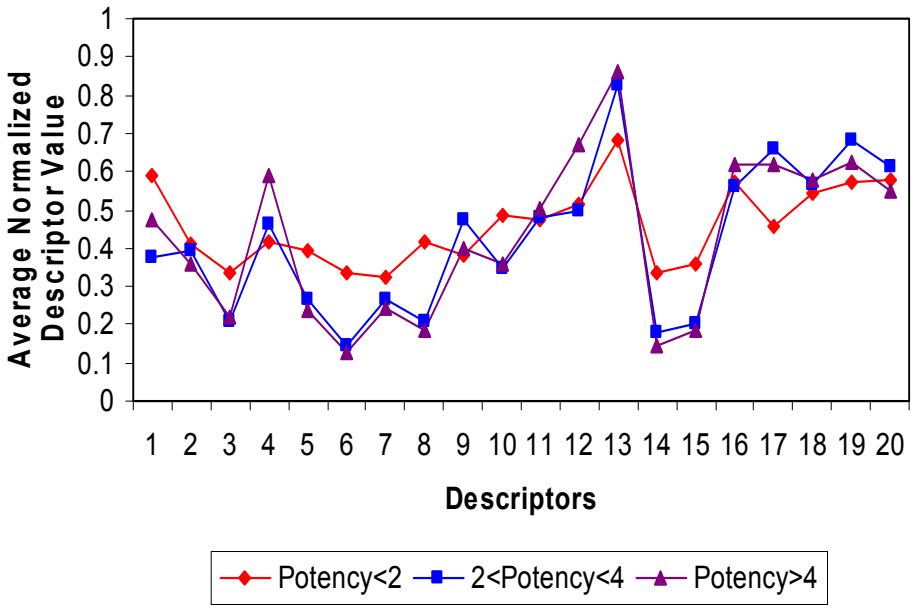

Therefore, it is reasonable to assume that the 'inductive' QSAR descriptors can effectively be used for the numerical quantification of the average potency of the CAMEL-s.

Composition of the training and the testing (validation) sets

In order to relate the 'inductive' descriptors to the experimental mean potencies of the peptides, we have employed the method of Artificial Neural Networks (ANN). Machine-learning approaches, particularly ANN, represent one of the essential parts of the modern QSAR, and the detailed description of the corresponding methodologies can be found elsewhere [e.g., in 46].

For this study, we chose the standard back-propagation configuration for the ANN and we used the Stuttgart Neural Network Simulator package [47] to implement the model. For effective training of the network (primarily to avoid overfitting), we used the training sets of 91 compounds randomly selected as 90 percent of the available CAMEL-s. Such random sampling has been performed 20 times and,

thus, 20 independent QSAR models have been created in order to evaluate the average predictive ability of the method. One of the training sets with 91 CAMEL peptides is presented in Table 2.

Table 2. Training Set of Camels in the 90/10 Split: the Mean Experimental Potencies vs. Predicted Potencies Using a Neural Network with Eight Hidden Nodes. The experimental potencies are average potencies against 24 Gram-positive and Gram-negative bacterial strains. The Camels are sorted according to ascending experimental potencies.

Identity	**Peptide sequence** (NH2 corresponds to the amidated C-terminus group)	**Experimental Potency**	**Predicted Potency**
CAMEL118	KWKLFLGILAVLKVL-NH2	0.159	0.335
CAMEL17	KWNLNGNINAVLKVL-NH2	0.209	0.176
CAMEL38	KWKGELEIEAELKVL-NH2	0.376	0.172
CAMEL107	GWKLGLKILNVLKVL-NH2	0.496	1.216
CAMEL20	KWKLFKKNNNNNKHN-NH2	0.498	1.490
CAMEL116	KWHLFLLILAVLKVL-NH2	0.514	0.405
CAMEL34	KRGLFKKGGAVLKGL-NH2	0.528	1.227
CAMEL18	KWHLRNKIGAVRNNL-NH2	0.537	1.183
CAMEL16	KHKLFKKIGAHRKRN-NH2	0.553	1.445
CAMEL39	HWHLHKHRGARHKVL-NH2	0.677	1.184
CAMEL134	GWELGEEILNVLKVL-NH2	0.708	0.160
CAMEL115	KWHLFLKILAVLKVL-NH2	0.741	1.646
CAMEL50	KWKLFKKHGNVRKVL-NH2	0.771	1.747
CAMEL10	KNKRNKKIGAVLKVL-NH2	0.848	1.216
CAMEL14	KHNLFKGIGAVLLVL-NH2	0.922	1.121
CAMEL51	KWKLFKKIGNRNKVL-NH2	0.947	1.631
CAMEL113	LWKLFLHILAVLKVL-NH2	0.962	0.162
CAMEL26	KNKLEKKIGAVLKVL-NH2	1.027	1.339
CAMEL52	KWKLGKGIGAVGKVL-NH2	1.033	1.080
CAMEL58	KWKLFNRIGHNRKVN-NH2	1.049	1.739
CAMEL137	GWRLFRGIRAVLNVL-NH2	1.074	0.296
CAMEL54	KWGLFKNIGAVLHVN-NH2	1.156	0.223
CAMEL57	RWKLNNNIGARLKVL-NH2	1.206	0.977
CAMEL33	HWKLFKKIGHVNKRL-NH2	1.34	1.937
CAMEL60	HWKRFLRIGHNLNVN-NH2	1.495	1.385
CAMEL11	KWKLFKKIGGVGGVL-NH2	1.593	2.133
CAMEL120	GWKLFLKILAVLKVL-NH2	1.598	0.785
CAMEL13	GWKLFKNRGAVLKHL-NH2	1.605	2.444
CAMEL8	KWKLFNKRGAVLKVL-NH2	1.605	2.404
CAMEL19	RWKNFKNIRANLRVL-NH2	1.742	2.017
CAMEL56	KWKLFGKNGRNLLVL-NH2	1.814	0.826
CAMEL138	GWRLFKGIRAVLNVL-NH2	1.826	1.157
CAMEL41	KWKLFKKGAVLKVLT-NH2	1.891	3.518
CAMEL47	KWKLFKKRNAVLKVL-NH2	1.964	2.497

Table 2. Cont.

Identity	**Peptide sequence** (NH2 corresponds to the amidated C-terminus group)	**Experimental Potency**	**Predicted Potency**
CAMEL44	KWKLFKKIGANLKVL-NH2	2.07	3.032
CAMEL12	KWKLFKRIGAVHKRL-NH2	2.242	1.675
CAMEL53	HWKLFKKIHAVRKHL-NH2	2.244	1.495
CAMEL112	KWKLFLHILAVLKVL-NH2	2.245	1.178
CAMEL32	KWKLFRKIGAVHRVL-NH2	2.306	2.906
CAMEL29	LWKLFKKHGAVLKVL-NH2	2.422	4.740
CAMEL36	KWHLNKRIHAVLKRL-NH2	2.587	2.129
CAMEL1	KWKLFKKGIGAVLKV-NH2	2.649	1.830
CAMEL35	KWKLFRRIGAVLKHR-NH2	2.706	1.816
CAMEL30	KRKRFRKIGAVLKVL-NH2	2.747	1.849
CAMEL15	KWKLFKLRGRVRKVL-NH2	2.879	3.728
CAMEL31	KWKLFKKIGLGLGVL-NH2	3.148	2.325
CAMEL2	KWKLFKKLKVLTTGL-NH2	3.246	3.974
CAMEL126	LWRLLKHILRVLKVL-NH2	3.259	3.974
CAMEL55	KWLLFKKIGAVLLNH-NH2	3.425	3.229
CAMEL37	LRKLFKKIRAVLLVR-NH2	3.617	3.407
CAMEL125	LWRLLKKILRVLKVL-NH2	3.822	4.820
CAMEL119	GWKLFKLIGAVLKVL-NH2	3.86	3.429
CAMEL28	KWKLGKKIGAVLGVL-NH2	3.946	3.055
CAMEL114	KWKLFHKILAVLKVL-NH2	4.105	4.843
CAMEL61	KWKLFKKAVLKVLTT-NH2	4.105	3.995
CAMEL111	KWKLFHLIGAVLKVL-NH2	4.165	3.484
CAMEL49	NWKLFHKIGAVLKVL-NH2	4.187	4.819
CAMEL25	KWKLRKKIGAVLKVL-NH2	4.262	3.762
CAMEL43	KWKGFKKIGAVLKVL-NH2	4.319	4.359
CAMEL105	GWKLGKKIGRVLKVL-NH2	4.336	5.555
CAMEL124	KWKLFKLIRAVLKVL-NH2	4.533	5.078
CAMEL7	KWKLFKKIGAVLHNL-NH2	4.534	3.614
CAMEL121	GWKGFKKIGRVLKVL-NH2	4.759	5.465
CAMEL27	KWKLFKKIGAVLNRL-NH2	4.869	4.987
CAMEL3	KWGLFKKIGAVLKVL-NH2	4.989	3.870
CAMEL81	KWKLFKKVLKVLTTG-NH2	5.297	4.455
CAMEL106	GWKLFKKIGRVLKVL-NH2	5.318	5.577
CAMEL127	GWKLFKKIGRVLRVL-NH2	5.47	5.130
CAMEL130	LWKLFKKIRRLLKVL-NH2	5.49	4.547
CAMEL128	LWKLFKKIGRVLKVL-NH2	5.493	5.375
CAMEL131	LWKLFRKIRRLLRVL-NH2	5.504	5.682
CAMEL104	GWKLGKKILRVLRVL-NH2	5.562	5.771
CAMEL108	KWKLGKKILNVLKVL-NH2	5.566	4.905
CAMEL109	GWRLGKKILRVLKVL-NH2	5.572	5.700
CAMEL123	LWKLFKKIRRVLRVL-NH2	5.614	5.656
CAMEL0	KWKLFKKIGAVLKVL-NH2	5.712	5.140
CAMEL42	HWKLFKKIGAVLKVL-NH2	5.712	4.706

Table 2. Cont.

Identity	**Peptide sequence** (NH2 corresponds to the amidated C-terminus group)	**Experimental Potency**	**Predicted Potency**
CAMEL102	GWKLGKKILRVLKVL-NH2	5.725	5.674
CAMEL6	NWKLFKKIGAVLKVL-NH2	5.803	5.205
CAMEL23	KWHLFKKIGAVLKVL-NH2	5.81	4.700
CAMEL101	KWKLGKKILRVLKVL-NH2	5.845	5.465
CAMEL103	GWKLGLKILRVLKVL-NH2	5.879	5.238
CAMEL22	GWKLFKKIGAVLKVL-NH2	5.946	5.363
CAMEL110	GWKLGKKILNVLKVL-NH2	6.043	5.637
CAMEL129	LWKLFKKINRVLKVL-NH2	6.045	5.212
CAMEL4	KWKLFHKIGAVLKVL-NH2	6.072	4.877
CAMEL24	KWKLFKHIGAVLKVL-NH2	6.167	4.880
CAMEL132	GWKLGKHILNVLKVL-NH2	6.182	5.035
CAMEL48	KWKLGKKIGAVLKVL-NH2	6.323	5.026
CAMEL136	VWRLIKKILRVFKGL-NH2	6.613	5.374
CAMEL135	GWRLIKKILRVFKGL-NH2	6.665	5.559

The remaining 10 polypeptides, featured in Table 3, were used as the corresponding testing group to access the method's predictive ability. For each polypeptide in the training and testing sets, we have transformed 20 network input descriptors into the normalized values varying from 0 to 1. Similarly, the output parameters from the ANN (mean antibacterial potencies) were normalized to [0:1] range.

Table 3. Validation (testing) Set of Camels in the 90/10 Split: Experimental Mean Potencies vs. Predicted Potencies by a Neural Network with Eight Hidden Nodes.

Identity	**A.A. Sequence**	**Experimental Potency**	**Predicted Potency**
CAMEL59	KGKGGKKGGRGGKVL-NH2	1.077	1.030
CAMEL40	GWLLHRNIGNVLHRL-NH2	1.387	1.167
CAMEL5	KWKLFKKNGAVLKVL-NH2	1.408	2.076
CAMEL139	GWKLFKGIRAVLNVL-NH2	1.497	1.524
CAMEL117	LWHLFLKILAVLKVL-NH2	1.515	0.194
CAMEL140	GWRLLKKILEVLKVL-NH2	4.136	1.203
CAMEL45	KWKNFKKIGAVLKVL-NH2	4.249	4.149
CAMEL122	LWKLFKKIRRVLKVL-NH2	6.142	5.593
CAMEL9	KWRLFKNIGAVLKVL-NH2	6.292	2.917
CAMEL46	KWKLFKGIRAVLKVL-NH2	6.45	4.825

QSAR model for CAMEL-s antibiotic potency

To quantify the antibacterial potencies of the CAMEL-s from the training sets, for each of them we built ANN consisting of 20 input, 8 hidden and 1 output nodes (as indicated on Figure 3).

Figure 3. Configuration of the Artificial Neural Network with 20 input, 8 hidden and 1 output nodes used in the study.

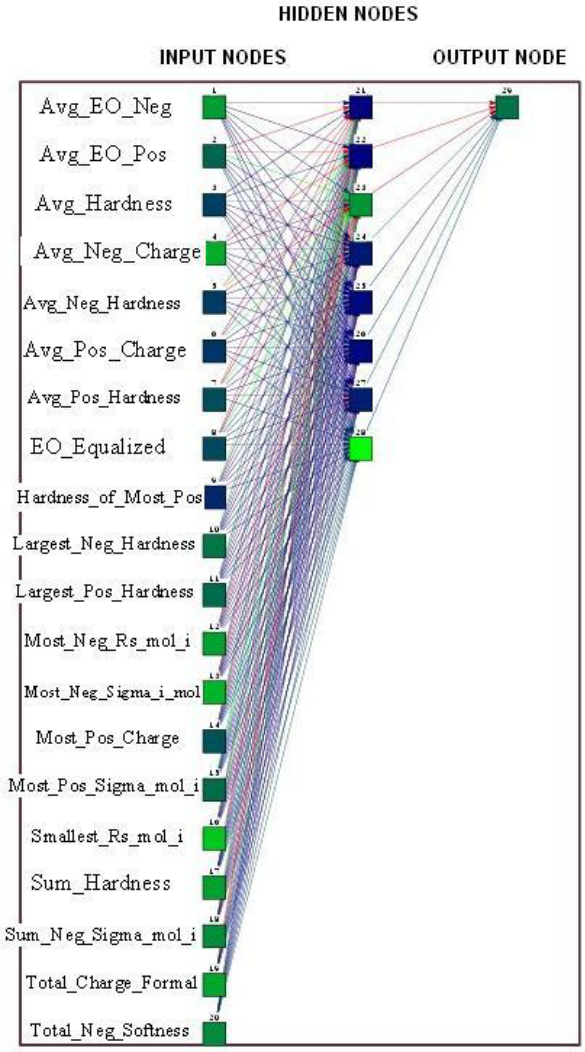

During the learning phase, the normalized values of the selected 20 'inductive' descriptors for each training peptide are fed to the ANN along with the experimental potencies. The relationship between the 20 input parameters and potency is established by recursively correcting the weights attributed to each parameter in such a way that the training potencies converge to the experimental potencies. The training was conducted with the learning rate of 0.8 and the learning update threshold of 0.2, while the input patterns were shuffled, and the initial weights were randomly assigned between 0 and 1. Random noise ranging from -0.002 to 0.002 was added to the ANN inputs to avoid the entrapment of the learning function in a local minimum. The theoretical antibacterial activities of 91 CAMEL-s from the representative training sample estimated during the learning phase are shown in Table 2 and plotted against the experimental numbers in Figure 4.

Figure 4. Predicted Potencies vs. Experimental Mean Potencies in the Training Set.

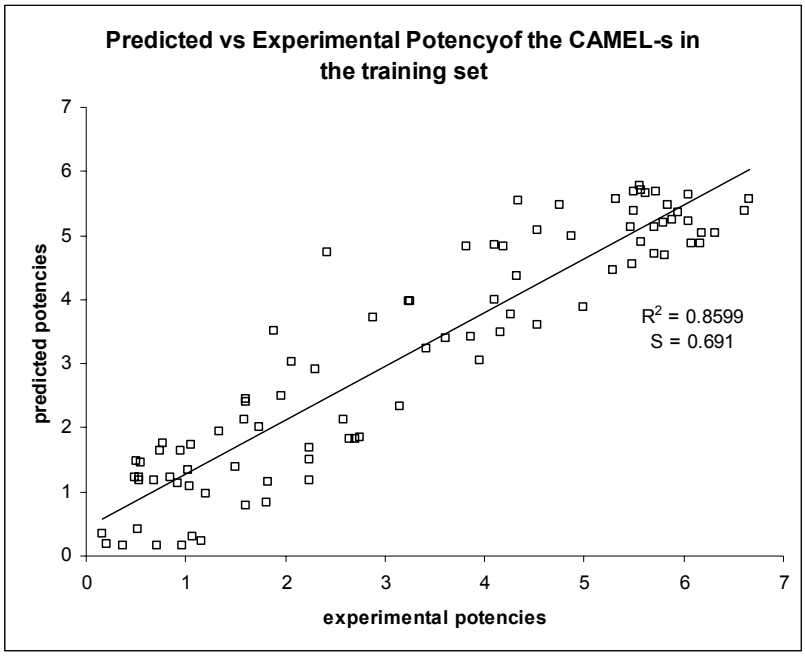

As it can be seen from the data, the 'inductive' descriptors allowed reproducing the average antibacterial activity of 91 CAMEL-s in the presented set of the training compounds with rather good accuracy. Considering that the examined potencies represent some averaged, not well standardized properties, the resulting QSAR predictions can be viewed as very adequate. To investigate the predictive power of the developed ANN-based solution, and to ensure that no overtraining occurred, we examined the network's performance on the testing compounds from Table 3. The normalized patterns of the independent variables for 10 CAMEL-s not used for the learning phase were passed through the trained ANN. The pre-estimated node–associated weights of the networks were used to compute the theoretical potencies of the validation compounds. The resulting output parameters collected in Table 3 demonstrate that with the exception of two peptides (CAMEL-s 9 and 140), the predicted CAMEL potencies accurately reproduce the experimental data, thereby validating the QSAR model generated here. It should be noted that similar ANN performance has been observed on all 20 training/testing random pairs of peptide datasets (the results for compounds from Tables 2 and 3 are actually one of the least accurate among the studied).

To assess the predictive ability of the developed approach in the categorical context (which is more appropriate for such non-standardized data with considerable uncertainty), we have also transformed the continuous outputs from the training and testing procedures into the discrete categorical format. Using the previously outlined conditional classification of the studied polypeptides, the performance of the neural network was assessed by comparing the categorical classification of the outputs from the neural network with the categories corresponding to the experimental potencies. For the cases in which the experimental potency and the predicted potency correspond to the same activity category the prediction of activity was considered to be correct.

Based on this simple assessment, the correct predictions by the developed QSAR model can be considered as 79% accurate for the presented training set (72 out of 91 CAMEL-s were correctly

assigned) and 80% accurate for the testing set in Table 3 (8 correct predictions out of 10). The significant deviations of the predicted potencies from the experimental potencies for two validation peptides – CAMEL 9 and CAMEL 140, indicate that the ANN-based approach underestimated the potency of these compounds.

Thus, the computed mean potency of CAMEL9 (2.917) is much lower than the corresponding experimental activity (6.292). This can, perhaps, be attributed to the non-exact character of the potency parameters and the model's discrepancies. Similarly, for CAMEL140, we predicted its potency to be 1.203 rather than 4.136. In this case, the error could be attributed to the very uncharacteristic composition of this peptide. It contains the negatively charged glutamic acid (E) residue which could not be adequately captured by the neural network which is trained on the set of peptides not containing this structural feature (only one peptide from the training set has E in the sequence). Despite the occasional misclassification, the developed ANN predictor has not missed by more than one class of antibacterial activity or, in other words, it did not place any peptides with high activity to the class of mild therapeutics and *vice versa*.

The accuracy of the created QSAR model can, possibly, be further improved by pre-processing the data for most adequate training and testing sets selection [48] or by using more powerful machine learning techniques. To summarize the section, it is possible to conclude, that the developed QSAR model operating by the 'inductive' descriptors and utilizing the ANN algorithm can accurately quantify the antibacterial potency of the studies synthetic cationic polypeptides and can effectively place them into groups of active, moderate and mild anti-infective compounds.

Conclusions and Further Directions

The evolution of bacterial strains into multi-drug resistant organisms progresses at an alarming rate. For this reason, it is crucial to discover novel non-specific antibiotics (such as cationic polypeptides) that are active against a number of different strains of microbes, including the resistant ones. The role of QSAR models for the antimicrobial polypeptides cannot be overestimated as such predictive solutions can significantly rationalize the selection, design and refinement efforts for these drugs. The developed QSAR approach utilizing the 'inductive' descriptors and based on the Artificial Neural Network algorithm can be used for these purposes and can be further expanded to cover a wider range of cationic peptides active against pathogens.

The approach can also be enhanced by utilizing purely statistical techniques in conjunction with the inductive QSAR descriptors which allows interpreting contributions from individual structural factors to the potency of the AMP-s. Despite the fact that the developed ANN-based method does not currently allow us to exactly evaluate the contributions of the individual QSAR descriptors, it is clear that the employed 'inductive' parameters adequately reflect those aspects of intra- and intermolecular interactions which govern antibacterial activity of the cationic polypeptides.

Hence, the developed methodology can further be applied to other important classes of cationic peptides, such as those active against viruses, fungi or tumours, and can provide excellent computational guidance for discovery of novel and potent therapeutic leads.

Acknowledgements

The authors thank Dr. David Wade for the CAMEL-s activity data and for useful suggestion in preparation of the manuscript.

References

1. Jaen-Oltra, J.; Salabert-Salvador, M.T.; Garcia-March, F.J.; Perez-Giminez, F.; Tomas-Vert, F. Artificial Neural Network Applied to Prediction of Fluorquinolone Antibacterial Activity by Topological Methods. *J. Med. Chem.* **2000**, *43*, 1143-1148
2. Garcia-Domenech, R.; de Julian-Ortiz, J.V. Antimicrobial Activity Characterization in a Heterogeneous Group of Compounds. *J. Chem. Inf. Comp. Sci*. **1998**, *38*, 445-449
3. Tomas-Vert, F.; Perez-Gimenez, F.; Salabert-Salvador, M.T.; Garcia-March, F.J.; Jaen-Oltra, J. Atrificial Neural Network Applied to the Discrimination of Antibacterial Activity by Topological Methods. *J. Molec. Struct. (Theochem).* **2000**, *504*, 249-259
4. Mishra, R.K.; Garcia-Domenech, R.; Galvez, J. Getting Discriminant Function of Antibacterial Activity from Physicochemical and Topological Parameters. *J. Chem. Inf. Comp. Sci*. **2001**, *41*, 387-393
5. Cronin, M.T.D.; Aptula, A.O.; Dearden, J.C.; Duffy, J.C.; Netzeva, T.I.; Patel, H.; Rowe, P.H.; Schultz T.W.; Worth, A.P.;, Voutzoulidis, K.; Schuurmann, G. Structure-Based Classification of Antibacterial Activity. *J. Chem. Inf. Comp. Sci*. **2002**, *42*, 869-878
6. Gozalbez, R., Galvez, J., Moreno, A., Garcia-Domenech, R. Discovery of New Antimalarial Compounds by use of Molecular Connectivity Techniques. *J. Pharm. Pharmacol.* **1999**, *51*, 111-117
7. Molina, E.; Diaz, H.G.; Gonzalez M.P.; Rodriguez, E.; Uriarte, E. Designing Antibacterial Compounds through a Topological Substructural Approach. *J. Chem. Inf. Comp. Sci*. **2004**, *44*, 515-521
8. Sima, P.; Trebichavsky, I.; Sigler, K. Mammalian antibiotic peptides. *Folia Microbiol.* **2003**, *48*, 123-137
9. Miele, R.; Bjorklund, G.; Barra, D.; Simmaco, M.; Engstrom, Y. Involvement of Rel factors in the expression of antimicrobial peptide genes in amphibian. *Eur. J. Biochem.* **2001,** *268*, 443-449
10. Simmaco, M.; Mignogna, G.; Barra, D. Antimicrobial peptides from amphibian skin: what do they tell us? *Biopolymers* **1998,** *47*, 435-450
11. Khush, R.S.; Leulier, F.; Lemaitre, B. Drosophila immunity: two paths to NF-κB. *Trends Immunol.* **2001,** *22*, 260-264
12. Hancock, R.E. Concerns regarding resistance to self-proteins. *Microbiology.* **2003,** *149*, 3343-3344
13. Marshall, S.H.; Arenas, G. Antimicrobial peptides: A natural alternative to chemical antibiotics and a potential for applied biotechnology. *Electron. J. Biotechno.* **2003,** *6*, 271-284
14. Hancock, R.E.; Chapple, D.S. Peptide Antibiotics. *Antimicrob. Agents Chemother.* **1999,** *43*, 1317-1323
15. Cherkasov, A.R.; Galkin, V.I.; Cherkasov, R.A. A New Approach to the Theoretical Estimation of Inductive Constants. *J. Phys. Org. Chem.* **1998**, *11*, 437-447

16. Cherkasov, A.R.; Galkin, V.I.; Cherkasov, R.A. "Inductive" Electronegativity Scale. *J. Molec. Struct. (Theochem)* **1999**, *489*, 43-46
17. Cherkasov, A.R.; Galkin, V.I.; Cherkasov, R.A. "Inductive" Electronegativity Scale. 2. "Inductive" Analog of Chemical Hardness. *J. Molec. Struct. (Theochem)* **2000**, *497*, 115-123
18. Cherkasov, A. Inductive Electronegativity Scale. Iterative Calculation of Inductive Partial Charges. *J. Chem. Inf. Comp. Sci*. **2003**, *43*, 2039-2047
19. Cherkasov, A., Sprous, D., Chen, R. 3D Correlation Analysis – New Method of Quantification of Substituent Effect. *J. Phys. Chem. A*. **2003**, *107*, 9695-9704
20. Cherkasov, A., Jonsson, M. Substituent Effect on Thermo-chemical Properties of Free Radicals. New Substituent Scales for C-Centred Radicals. *J. Chem. Inf. Comp. Sci*. **1998**, *38*, 1151-1156
21. Cherkasov, A., Jonsson, M. Substituent Effect on Thermochemical Properties of Free Radicals. Physical Interpretation of the Substituent Effect. *J. Chem. Inf. Comp. Sci*. **1999**, *39*, 1057-1063
22. Cherkasov, A.R., Jonsson, M., Galkin, V.I. A Novel Approach to the Analysis of Substituent Effects. Quantitative Interpretation of Ionization Potentials and Gas Basicity of Amines. *J. Mol. Graph. Model.* **1999**, *17*, 28-43
23. Cherkasov, A., Jonsson, M. Estimation of Homolytic CH Bond Dissociation Enthalpies. *J. Chem. Inf. Comp. Sci*. **2000**, *40*, 1222-1226
24. Galkin, V.I., Cherkasov, A.R., Cherkasov, R.A. Modelling of Substituents Electronic and Steric Effects. Effective Analysis of Organoelement and Organophosphorus Reactivity. *Phosphorus, Silicon, Sulphur.* **1999**, *146*, 329-332
25. Cherkasov, A. Inductive QSAR Descriptors. 1. Distinguishing Compounds with Antibacterial Activity by Artificial Neural Networks. Submitted *J. Chem. Inf. Comp. Sci.* **2004,** *44*
26. Mee, R.P.; Auton, T.R.; Morgan, P.J. Design of active analogs of a 15-residue peptide using D-optimal design, QSAR and a combinatorial search algorithm. *J. Pept. Res.* **1997**, *49*, 89-102
27. Edlund, C.; Hedberg, M.; Engström, Å.; Flock, J.-I.; Wade, D. Anti-anaerobic activity of a cecropin-melittin peptide.Clin. Microbiol. *Infection* **1998**, *4*, 181-185
28. Oh, H.; Hedberg, M.; Wade, D.; Edlund, C. Activities of synthetic hybrid peptides against bacteria: aspects of methodology and stability. *Antimicrob. Agents Chemother.* **2000**, *44*, 68-72
29. Oren, Z.; Shai, Y. Mode of action of linear amphipathic α-helical antimicrobial peptides. *Biopolymers* **1999**, *47*, 451-463
30. Bechinger, B. The structure, dynamics and orientation of antimicrobial peptides in membranes by multidimensional solid-state NMR spectroscopy. *Biochim. Biophys. Acta* **1999**, *1462*, 157-183
31. Blondelle, S.E.; Lohner, K.; Aguilar, M.I. Lipid-induced conformation and lipid-binding properties of cytolytic and antimicrobial peptides: determination and biological specificity. *Biochim. Biophys. Acta* **1999**, *1462*, 89-108
32. Epand, R.F.; Umezawa, N.; Porter, E.A.; Gellman, S.H.; Epand, R.M. Interactions of the antimicrobial β-peptide β-17 with phospholipids vesicles differ from membrane interactions of magainins. *Eur. J. Biochem.* **2003**, *270*, 1240-1248
33. Hancock, R.E.; Lehrer, R. Cationic peptides: a new source of antibiotics. *Trends Biotechnol.* **1998**, *16*, 82-88
34. Shai, Y. Mechanism of the binding, insertion and destabilization of phospholipids bilayer membranes by α-helical antimicrobial and cell non-selective membrane-lytic peptides. *Biochim. Biophys. Acta* **1999**, *1462*, 55-70

35. Takeshima, K.; Chikushi, A.; Lee, K.K.; Yonehara, S.; Matsuzaki, K. Translocation of analogues of the antimicrobial peptides magainin and buforin across human cell membranes. *J. Biol. Chem.* **2003**, *278*, 1310-1315
36. Vogt, T.C.B.; Bechinger, B. The interactions of histidine-containing amphipathic helical peptide antibiotics with lipid bilayers. *J Biol. Chem.* **1999**, *274*, 29115-29121
37. Baker, M.A.; Maloy, W.L.; Zasloff, M.; Jacob, L.S. Anticancer efficacy of Magainin2 and analogue peptides. *Cancer Res.* **1993**, *53*, 3052-3057
38. Dathe, M.; Schumann, M.; Wieprecht, T. Peptide helicity and membrane surface charge modulate the balance of electrostatic and hydrophobic interactions with lipid bilayers and biological membranes. *Biochemistry* **1996**, *35*, 12612-12622
39. Dathe, M.; Wieprecht, T. Structural features of helical antimicrobial peptides: their potential to modulate activity on model membranes and biological cells. *Biochim. Biophys. Acta* **1999,** *1462*, 71-87
40. Epand, R.M.; Vogel, H.J. Diversity of antimicrobial peptides and their mechanisms of action. *Biochim. Biophys. Acta* **1999,** *1462*, 11-28
41. Hwang, P.M.; Vogel, H.J. Structure-function relationships of antimicrobial peptides. *Biochem. Cell Biol.* **1998,** *76*, 235-246
42. Peck-Miller, K.A.; Blake, J.; Cosand, W.L.; Darveau, R.P.; Fell, H.P. Structure-activity analysis of the antitumor and hemolytic properties of the amphiphilic alpha-helical peptide, C18G. *Int. J. Pept. Prot. Res.* **1994,** *44*, 143-151
43. Prenner, E.J.; Lewis, R.N.A.H.; McElhaney, R.N. The interaction of the antimicrobial peptide gramicidin S with lipid bilayer model and biological membranes. *Biochim. Biophys. Acta* **1999,** *1462*, 201-221
44. Shin, S.Y.; Lee, S.H.; Yang, S.T.; Park, E.J.; Lee, D.G.; Lee, M.K.; Eom, S.H.; Song, W.K.; Kim, Y.; Hahm, K.S.; Kim, J.I. Antibacterial, antitumor and hemolytic activities of alpha-helical antibiotic peptide, P18 and its analogs. *J. Pept. Res.* **2001,** *58*, 504-514
45. Chemical Computation Group Inc., Montreal (Canada). *Molecular Operational Environment*, **2004**
46. Zupan, J.; Gasteiger, J. *Neural Networks in Chemistry and Drug Design, 2nd Ed.*; Wiley: New York, **1999**
47. SNNS: Stuttgart Neural Network Simulator; Version 4.0, University of Stuttgart, Stuttgart (Germany), **1995**
48. Hawkins, D.; Basak, S.; Mills, D. Assessing Model Fit by Cross Validation. *J. Chem. Inf. Comp. Sci*., **2003**, *43*, 579-586